

The Voyager 2 Encounter with the Neptunian System

E. C. STONE AND E. D. MINER

An overview of the Voyager 2 encounter with Neptune is presented, including a brief discussion of the trajectory, the planned observations, and highlights of the results described in the 11 companion papers. Neptune's blue atmosphere has storm systems reminiscent of those in Jupiter's atmosphere. An optically thin methane ice cloud exists near the 1.5-bar pressure level, and an optically thick cloud exists below 3 bars. Neptune's magnetic field is highly tilted and offset from the planet's center; it rotates with a period of 16.11 hours. Two narrow and two broad rings circle the planet; the outermost of these rings has three optically thicker arc segments. Six new moons were discovered in circular prograde orbits, all well inside Triton's retrograde orbit. Triton has a highly reflective and geologically young surface, a thin nitrogen atmosphere, and at least two active geyser-like plumes.

MORE THAN A DOZEN YEARS AFTER its 20 August 1977 launch from Cape Canaveral, Florida, Voyager 2 completed its fourth and final planetary encounter (1). Before the closest approach of Voyager 2 to Neptune, both Voyager 1 and Voyager 2 had completed successful encounters with Jupiter [closest approaches, 5 March and 9 July 1979, respectively (2)] and with Saturn [closest approaches, 12 November 1980 and 26 August 1981, respectively (3)]. Voyager 2 continued on to successful encounters with Uranus on 24 January 1986 (4) and with Neptune on 25 August 1989. This and the following reports summarize the initial findings from the investigations conducted during the Voyager 2 passage through the Neptunian system. An earlier paper (5) reported Neptune's wind speeds on the basis of early imaging results.

The investigations and principal investigators are listed in Table 1. All instruments and engineering systems, including the science instrument scan platform and the spacecraft radio receiver, functioned nominally during the encounter with Neptune. Although contingency backup sequences and procedures were prepared in the event of scan platform seizure and other problems, none of these was required during the encounter.

E. C. Stone, Division of Physics, Mathematics, and Astronomy, California Institute of Technology, Pasadena, CA 91125.
E. D. Miner, Jet Propulsion Laboratory, California Institute of Technology, Pasadena, CA 91109.

Several improvements were made to the spacecraft and ground systems since the 1986 Uranus encounter. Attitude control was altered to further reduce angular rates by about 25% below those experienced at Uranus, to further improve compensation for impulses from tape recorder starts and stops, to permit an additional scan platform rate useful for motion compensation near closest approaches to Neptune and Triton, and to provide for "nodding" image motion compensation (NIMC). NIMC permitted acquisition of motion-compensated images without disrupting the communication link with Earth or utilizing limited tape recorder resources. Instrument control for the imaging system was also changed to permit expo-

sure durations between 15 and 96 s, and real-time images with exposure durations in multiples of 48 s, capabilities used extensively during the encounter at Neptune, where light levels were only 40% of those at Uranus.

The greater distance of Neptune also resulted in lower Voyager signal strengths at Earth-based tracking stations. Each of the three 64-m-diameter tracking antennas of the National Aeronautics and Space Administration (NASA) Deep Space Network (DSN) were enlarged to 70-m diameter and improved in shape. A high-efficiency, 34-m tracking station was added to the Madrid DSN complex. Extensive arraying of antennas was used to further increase the effective collector area. The 64-m Parkes Radio Telescope in Australia was again made available to enhance the capability of the Canberra DSN tracking antennas. Similarly, Voyager signals collected by the National Radio Astronomy Observatory's Very Large Array (VLA) near Socorro, New Mexico, were combined with signals collected at the Goldstone (California) DSN complex. The 27 25-m antennas of the VLA provide a collecting area equivalent to two 70-m antennas. During closest approach operations on 25 August, the Japanese Institute of Astronomical Science utilized its 64-m tracking antenna at Usuda, Japan, to augment Voyager radio science data collection. The spacecraft and all of the ground systems worked flawlessly during the Neptune encounter, again testifying to the high level of expertise and teamwork within the Voyager project and its supporting organizations.

Neptune encounter planning. With no future planetary encounters on the Voyager itinerary, project personnel were free to design the trajectory and timing to maximize the science return during the Neptune-Triton encounter. Three primary objectives were

Table 1. Voyager investigations and principal investigators.

Investigation	Principal investigator and affiliation
Imaging (ISS)	B. A. Smith, University of Arizona, Tucson, AZ
Photopolarimetry (PPS)	A. L. Lane, Jet Propulsion Laboratory, California Institute of Technology, Pasadena, CA
Infrared spectroscopy (IRIS)	B. J. Conrath, Goddard Space Flight Center, Greenbelt, MD
Ultraviolet spectroscopy (UVS)	A. L. Broadfoot, University of Arizona, Tucson, AZ
Radio science (RSS)	G. L. Tyler, Stanford University, Stanford, CA
Magnetometry (MAG)	N. F. Ness, Bartol Research Institute, University of Delaware, Newark, DE
Plasma (PLS)	J. W. Belcher, Massachusetts Institute of Technology, Cambridge, MA
Low-energy charged particles (LECP)	S. M. Krimigis, Applied Physics Laboratory, The Johns Hopkins University, Laurel, MD
Cosmic rays (CRS)	E. C. Stone, California Institute of Technology, Pasadena, CA
Plasma waves (PWS)	D. A. Gurnett, University of Iowa, Iowa City, IA
Planetary radio astronomy (PRA)	J. W. Warwick, Radiophysics, Inc., Boulder, CO

met by the encounter: (i) a close approach to Triton, including both sun and Earth occultations as viewed from the spacecraft; (ii) a close polar passage of Neptune, including both sun and Earth occultations; and (iii) timing of closest approach such that both of the Neptune-Triton occultations occurred at relatively high elevation angles over the Canberra DSN complex. The spacecraft trajectory through the Neptune system is shown in Fig. 1.

Voyager 2 encounter activities commenced on 5 June 1989, with the spacecraft 117×10^6 km from Neptune. Closest approach, at 29,240 km from the center of Neptune, occurred at 0356 UTC (coordinated universal time) on 25 August 1989. Radio signals beamed by Voyager 2 at that time reached Earth 4 hours 6 min later. A Triton closest approach occurred at 0910 UTC at a distance of 39,800 km from the center of this largest satellite of Neptune. The encounter period ended on 2 October 1989.

The design of the Neptune science sequences relied primarily on telescopic observations from Earth and on Voyager findings at Uranus, although some early Voyager data were used to make revisions to later observations. Provision was made for late retargeting of imaging frames to newly discovered satellites and rings. Timing of close Neptune and Triton observations was also adjusted at the last possible moment to take advantage of the most recent estimates of geometric event times made by the navigation team.

Ring occultations of σ Sagittarii were observed by the photopolarimeter (PPS) and the ultraviolet spectrometer (UVS). Radio science (RSS) data were collected in Australia and Japan during a 7-hour period that included occultations of the spacecraft signal by the rings, the planet, and Triton. Solar occultations of these same bodies were recorded by the UVS. An occultation by Triton of β Canis Majoris was recorded by the UVS and the PPS. The temperature of Neptune's atmosphere was mapped with the infrared spectrometer (IRIS), and PPS, IRIS, UVS, and imaging (ISS) were used to determine the scattering, emitting, and reflecting characteristics of the atmosphere under various viewing conditions. Ring images were obtained on approach to the planet, during passage of the spacecraft through the shadow of Neptune, near the time of outbound ring plane crossing, and while the spacecraft was receding from the nightside of the planet.

Extensive searches for new satellites were conducted by ISS, both inside and outside the expected ring system. The spacecraft was rolled to three specific orientations to en-

hance plasma (PLS) and low-energy charged particle (LECP) observations of corotating ions during the inbound and outbound legs of the trajectory and of precipitating charged particles over Neptune's north polar region near the time of closest approach. Detailed imaging and nonimaging observations of Triton occupied all of the time period from 2 to 8 hours after Neptune's closest approach. High-rate plasma wave (PWS) and planetary radio astron-

omy (PRA) data were recorded to search for tiny ring particles near the times of both ring plane crossings (63 minutes before and 79 minutes after closest approach); a series of high-rate PWS frames was also recorded during passage over the north polar region of the planet. The magnetosphere and its charged-particle population were observed continuously by the magnetometer (MAG), cosmic ray (CRS), LECP, and PLS exper-

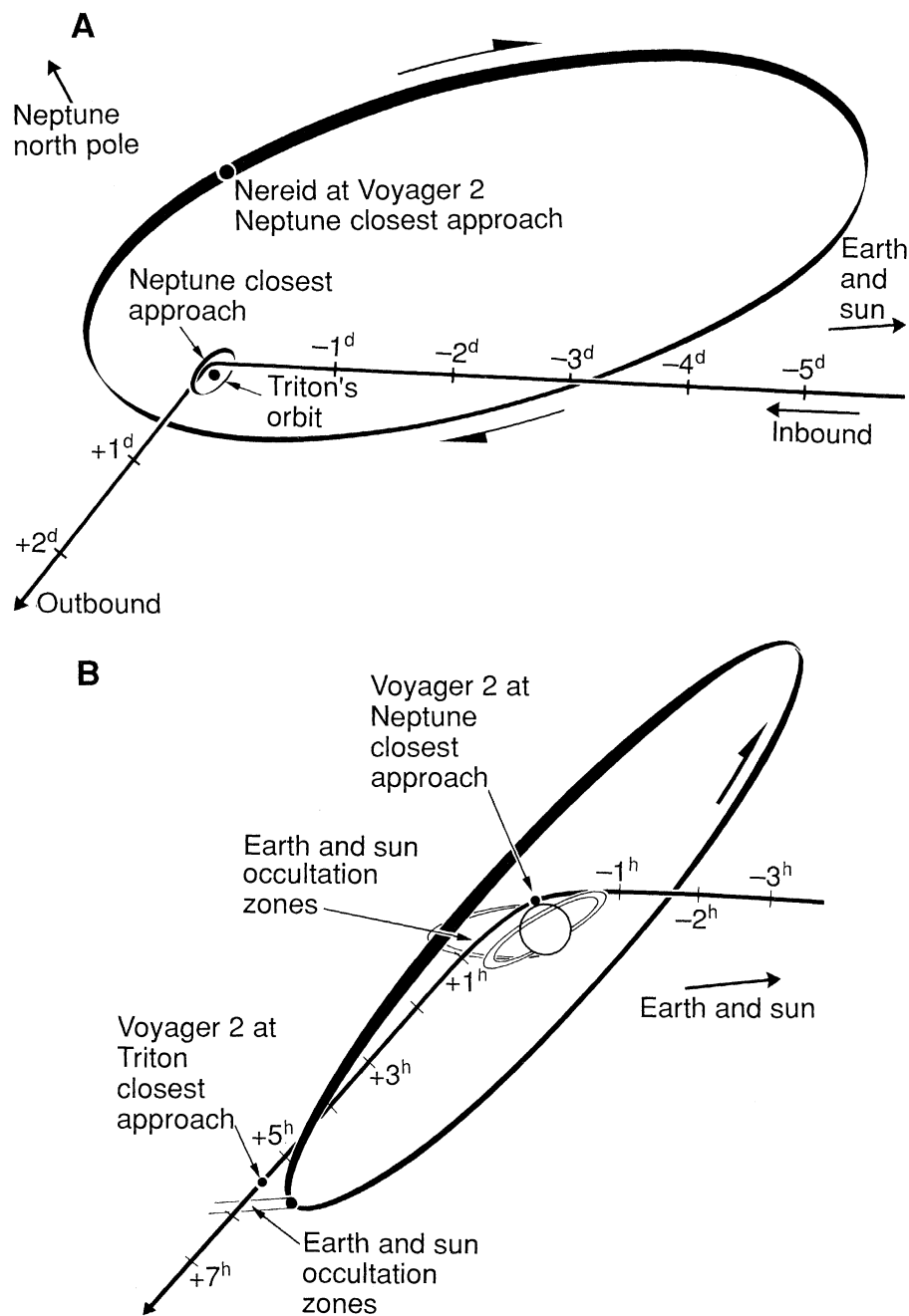


Fig. 1. The Voyager 2 path through the Neptune system is shown in the plane of the spacecraft trajectory. (A) The projected orbits of Triton and Nereid are shown, together with the positions of these satellites at the time of Voyager 2's closest approach to Neptune. Tick marks along the trajectory indicate Voyager's position at 1-day intervals. (B) An enlarged view covers a 10-hour period that includes closest approaches to Neptune and Triton and passage through Earth and solar shadows (occultation zones) of each. Tick marks along the trajectory are at 1-hour intervals.

Atmosphere. Neptune has an effective temperature of about 59.3 K. Derivation of Neptune's Bond albedo will require more detailed analysis of IRIS, PPS, and ISS data, but the effective temperature implies that Neptune emits about 2.7 times as much energy as it absorbs from the sun. This greater contribution of internal heat may be the cause of the greater activity of Neptune's atmosphere relative to that of Uranus. Although solar heating is greater in the equatorial region of Neptune and in the polar regions of Uranus, the horizontal temperature structures of the two atmospheres are remarkably similar, with poles and equator at very nearly equal temperatures and mid-latitudes several degrees cooler. A minimum temperature of about 50 K is found near the 100-mbar pressure level. A multilayer ionosphere is found at altitudes of 1000 to 4000 km above 1 bar. Temperatures in the extreme upper atmosphere are near 750 K, but, because of Neptune's larger mass, colder thermosphere, and greater ring distances, the effects of gas drag on ring material are less at Neptune than at Uranus.

As with all the giant planets, hydrogen (H_2) is the dominant atmospheric constituent. A precise determination of the mole fraction of atmospheric helium $[He]/[H_2]$ is not yet available, but it is less than 0.25. Methane (CH_4) is more abundant in Neptune's upper atmosphere (0.01 to 0.1 μ bar) than at Uranus, with $[CH_4]/[H_2]$ near 3×10^{-5} . The absorption of red light by CH_4 gives Neptune its characteristic blue color. Somewhat deeper in the atmosphere (about 1.5 mbar), acetylene (C_2H_2) was detected with a mole fraction of 10^{-7} to 10^{-6} . The signature of an optically thin cloud deck of CH_4 ice was seen in radio occultation data below 1.2 bar, but analysis to date leads only to a lower limit of 1% on the CH_4 mole fraction beneath that cloud. Strong absorption of radio waves may indicate the presence of small amounts of ammonia (NH_3). Pre-Voyager models predicted a cloud of hydrogen sulfide (H_2S) at a level of several bars, but H_2S is too transparent to radio waves to account for the observed absorption.

Several prominent cloud features are apparent in images of Neptune's atmosphere. These include an Earth-sized "Great Dark Spot" (GDS) near -20° latitude reminiscent in relative size and latitude of Jupiter's Great Red Spot. The GDS rolls in an anticyclonic (counterclockwise) direction with a 16-day period. A smaller dark spot with a bright central core is located at -55° latitude. Bands of lower reflectivity extend from $+6^\circ$ to $+25^\circ$ latitude and from -45° to -70° latitude. Bright cirrus-like cloud features flank the GDS; other similar features

Table 2. Neptune ring data.

Feature	Distance (10^3 km)	Distance (R_N)	Width (km)	Optical depth	Comments
1-bar atmosphere	24.76	1.000			Equatorial radius of Neptune
	38.	1.5		<0.0001	Inner extent of 1989N3R?
1989N3R	41.9	1.69	1700*	0.0001	High dust content
	49.	2.0		<0.0001	Outer extent of 1989N3R?
1989N2R	53.2	2.15	†	0.01	High dust content
1989N4R (inner)	53.2	2.15		0.0001	Inner edge of "plateau"
1989N4R (outer)	59.	2.4		0.0001	Outer edge of "plateau"
1989N1R	62.9	2.54	15	0.01–0.1	Contains three bright dusty arcs

*Tabulated width of 1989N3R is full width at half maximum. †1989N2R is narrow and unresolved in Voyager images.

occupy relatively narrow latitude ranges near latitudes of $+27^\circ$ and -71° . These are thought to be optically thick upward extensions of the CH_4 cloud deck; their detailed appearance changes with time scales that are small as compared with the 16-hour rotation period. The "Scooter" is a bright feature near -42° latitude that is deeper in the atmosphere than the cirrus clouds and may be an upward extension of the deeper cloud deck.

These large-scale atmospheric features move at wind speeds ranging from about $+20$ $m\ s^{-1}$ (prograde) at -54° latitude to -325 $m\ s^{-1}$ (retrograde) at -22° . Velocities are measured with respect to the internal rotation of Neptune, which has a period of 16.11 hours as determined from periodic radio emissions. The GDS resides in a region with strong wind shears. It undoubtedly lies at a lower level than most of the brighter cloud features measured, and the presence of orographic ("lee") clouds near its western boundary implies that it is an impediment to the higher altitude winds. Shadows cast by higher CH_4 clouds on a lower cloud deck show that the cirrus-like clouds are located at altitudes of 50 to 100 km above the lower cloud layer. Optically thin haze layers produced photochemically from CH_4 lie at still higher altitudes.

The ultraviolet spectrum of the sunlit atmosphere is dominated by Lyman α emission from atomic hydrogen. The 340-rayleigh intensity almost perfectly matches the galactic background radiation, and unambiguous detection of the planet in ultraviolet light was consequently difficult. The temperature of the extreme upper atmosphere is 750 ± 150 K. This value is close to that observed at Uranus, but Neptune's higher gravity and somewhat colder stratosphere combine to yield much lower number densities in Neptune's upper atmosphere than were seen at Uranus.

Weak auroral emissions radiating 5×10^7 W have been tentatively identified on the nightside of Neptune near longitudes of 30° and 200° .

Rings. Earth-based stellar occultation measurements during the early and middle

1980s seemed to imply the presence of partial rings (ring arcs) at several radial distances from Neptune's center (6). Voyager found a system of prograde, equatorial, circular rings (Table 2). The outermost of these rings, at a distance of 62,900 km from the planet's center, includes three optically thicker "arcs" extending 4° , 4° , and 10° in ring longitude. These arcs are believed to be responsible for all but one of the confirmed ring occultation events seen from Earth. The remaining event was apparently a chance occultation of 1989N2, the second of the Neptune satellites discovered by Voyager.

Narrow rings are thought to be confined by the actions of relatively nearby satellites. 1989N4 and 1989N3 orbit just inside the two narrow rings, 1989N1R and 1989N2R, respectively, and may serve to prevent ring material from spiraling inward toward Neptune. No ring shepherds (satellites) have been found at the outer edges of these rings, although satellites with diameters of ≤ 12 km would have escaped detection. It is not presently known whether additional smaller shepherding satellites exist or if other confinement mechanisms are at work. The brighter arcs within 1989N1R are also an enigma. Such material, if azimuthally unrestrained with the ring, should spread relatively evenly around the ring within only a few years.

Particle sizes within the rings appear to be smaller than was the case with the Uranus rings. The rings were not readily detected by the radio occultation experiment, although additional processing of the data may yield useful ring information. Stellar occultation measurements by PPS and UVS revealed 1989N1R. It should be noted that σ Sagittarii passed behind the leading 4° arc of 1989N1R; Voyager 2 did not pass behind any of the ring arcs in 1989N1R during the radio occultation experiment. The central core of the ring was 10 km in radial width, consistent with imaging measurements. There was a marginal detection of 1989N2R by PPS. Comparison of high-phase and low-phase images of the rings shows that the dust content of 1989N2R

and 1989N3R is about twice that of the other rings and much more than that of the main rings of Saturn and Uranus. The three arcs also seem to have more dust than the remainder of 1989N1R.

Particle impacts detected at both ring plane crossings are indicative of a thousand-kilometer-thick region of micrometer-sized particles. Impact rates reached a maximum of about 280 s^{-1} during the inbound crossing at 85,500 km from the planet center; rates at the outbound crossing (103,700 km) peaked at about 110 s^{-1} . These rates imply a number density of order 10^{-3} m^{-3} . Significant but lower count rates were detected more than 20,000 km above and below the ring plane, as well as over the northern polar region.

Satellites. Six new satellites were found in Voyager images during approach to the planet. All orbit the planet in prograde, circular orbits of low inclination. The orbital and physical characteristics of Neptune's eight known satellites are given in Table 3. Five of the six newly discovered satellites orbit within 1° of Neptune's equatorial plane. 1989N6 has an inclination close to 5° . Combined Earth-based and Voyager observations show Triton's inclination to be 157° , whereas Nereid's orbit inclination is a more moderate 29° . The respective orbital eccentricities of Triton and Nereid are 0.00 and 0.75; Nereid's distance from Neptune's center varies from 1.39×10^6 to 9.64×10^6 km. Triton orbits in synchronous rotation, with the same side always facing the planet; the regular satellites (prograde orbit, low inclination) discovered by Voyager probably share this characteristic. Nereid's highly elliptical orbit makes it theoretically unlikely that its rotation and orbital periods are equal. However, no rotational brightness variations in excess of 10% were detected, and Nereid's rotation period remains unknown.

The mass of the Neptune system, expressed as the product of the mass and the universal gravitational constant (G), was found from radio tracking to be $6,836,534 \pm 20 \text{ km}^3 \text{ s}^{-2}$. The mass of Triton is $1428.5 \pm 4.5 \text{ km}^3 \text{ s}^{-2}$; the corresponding density is $2.07 \pm 0.02 \text{ g cm}^{-3}$. Subtracting the mass of Triton and an additional $10 \text{ km}^3 \text{ s}^{-2}$ for the small satellites and rings yields a Neptune mass of $6,835,096 \pm 21 \text{ km}^3 \text{ s}^{-2}$ and a mean density of 1.64 g cm^{-3} .

As may be seen from the best resolutions (in kilometers per line pair) in Table 3, the disks of all eight satellites were resolved in the best images. Nevertheless, the diameters in Table 3 for the three inner satellites are calculated on the assumption that their surface reflectivities are consistent with the 5 to

Table 3. Neptune satellite data.

Satellite name	Distance (10^3 km)	Distance (R_N)	Period (hours)	Diameter (km)	Resolution (km per line pair)	Normal albedo
1989N6	48.0	1.94	7.1	54 ± 16	47.2	0.06?
1989N5	50.0	2.02	7.5	80 ± 16	34.8	0.06?
1989N3	52.5	2.12	8.0	180 ± 20	36.8	0.06?
1989N4	62.0	2.50	10.3	150 ± 30	33.8	0.054
1989N2	73.6	2.97	13.3	190 ± 20	8.2	0.056
1989N1	117.6	4.75	26.9	400 ± 20	2.6	0.060
Triton	354.8	14.33	141.0	2705 ± 6	0.8	0.6–0.9
Nereid	5513.4	222.65	8643.1	340 ± 50	86.6	0.14

6% normal albedos of 1989N1 through 1989N3. Surface features may be seen in the best images of 1989N1 and 1989N2, both of which appear to be heavily cratered and nonspherical. Some of the other small satellites may be fragments of earlier larger satellites.

Triton has the lowest observed surface temperature of any natural body in the solar system: $38 \pm 4 \text{ K}$. Its atmosphere is predominantly nitrogen (N_2), but CH_4 is also present in the lower atmosphere with a mixing ratio of about 10^{-4} . The surface pressure as measured by RSS is $16 \pm 3 \text{ } \mu\text{bar}$. A thermal inversion may exist in the lower 5 km of the atmosphere, and a tropopause altitude of 25 to 50 km is inferred. It is uncertain whether the clouds and haze layers observed in this region of the atmosphere result from simple condensation or from surface eruptions. The temperature at altitudes above 400 km is $95 \pm 5 \text{ K}$. Atmospheric N_2 is transported from the illuminated polar regions to the unilluminated polar regions.

Triton's surface appears to be geologically young and devoid of heavily cratered terrain. A covering of seasonal ice (probably N_2) dominates the polar regions south of latitude -15° (spring in Triton's southern hemisphere extends from about 1960 to the year 2000). This seasonal ice has a slight reddish tint, possibly due to the presence of organic compounds produced from CH_4 and N_2 by the actions of photochemistry and energetic particle bombardment. A thin layer, perhaps of fresh N_2 frost, occupies the equatorial regions of Triton at most longitudes. This layer appears as a bright, slightly blue coloration, which does not obscure the underlying topography. Northward of the equator the surface has a variety of terrain types; the most widespread of these is reminiscent of the skin of a cantaloupe.

"Cantaloupe" terrain dominates the western (trailing) hemisphere of Triton and consists of a dense concentration of pits or dimples that are crisscrossed by ridges. Few impact craters are discernible in these areas. The eastern (leading) hemisphere consists of

a series of much smoother units, including caldera-like structures of water ice. These frozen lakes are surrounded by successive terraces, indicative of multiple epochs of flooding. All of Triton's surface features are apparently overlain by a relatively thin veneer of CH_4 and N_2 ices and their derivatives. All of Triton's surface appears to be geologically young; however, features in the eastern half of the Neptune-facing hemisphere are relatively more heavily cratered and hence older.

Within the polar regions are large numbers of wind streaks with albedos 10 to 20% lower than the polar ices. Because the streaks seem to overlie deeper ice deposits, it is likely that they are younger than 1000 years or so. Indeed, two active geyser-like plumes were discovered near the subsolar latitude (-55°). Each rises vertically to an altitude of about 8 km, as determined from stereoscopic viewing. There a dense cloud of material forms; this cloud serves as a source for a westward wind-driven trail of material more than 100 km long. The plume shadow is discernible in high-resolution oblique views. These plumes may result from the explosive release of N_2 gas, which carries ice-entrained dark material in the exit nozzle to high altitudes.

Its inclined retrograde orbit implies that Triton is a captured object, initially formed independently of Neptune (like Pluto) in the outer solar system (7). Eventually it wandered too close to Neptune and either collided with an existing satellite or was slowed by gas drag sufficiently to be captured into an eccentric and inclined retrograde orbit. Tidal forces from Neptune circularized the orbit and kept Triton molten for much of its early history. Preexisting surface features were destroyed, and complete differentiation probably occurred. Its density suggests that a silicate core may occupy the inner 1000 km of Triton's radius. Radiogenic heating from this silicate core and from subsequent meteoritic infall may have provided energy for the melting and remelting of surface ice to form the observed calderas, for the more viscous ice

eruptions along surface fractures, and possibly also for the observed wind streaks and active plumes.

Magnetosphere. The first direct indication of a Neptune magnetic field was obtained from radio emissions detected 8 days before closest approach, at a distance of about 470 Neptune radii (R_N). Voyager subsequently crossed a well-defined, detached bow shock at 34.9 R_N . The inbound magnetopause was less well-defined, because Voyager entered a highly tilted magnetic field at very high magnetic latitude, permitting the first observations of a "pole-on" magnetosphere in which the solar wind is incident on the magnetic polar region rather than the equatorial. A gradual crossing occurred between 26.5 and 23.0 R_N . Close to the planet (within 4 R_N), the magnetic field is poorly represented by an offset tilted dipole (OTD); between 4 and 15 R_N the field may be represented as a dipole tilted 46.8° with respect to the rotation axis and offset 0.55 R_N into the southern hemisphere and away from the rotation axis of Neptune. The dipole moment is 0.133 G- R_N^3 , but, because of the large offset, the surface field represented by the OTD model is highly asymmetric, varying from a maximum of >1.0 G in the southern hemisphere to a minimum of <0.1 G in the northern hemisphere.

As the magnetic field rotates with the planet each 16.11 hours, satellites and ring particles sweep through large ranges of magnetic latitude and L -shell values. The incident solar wind deforms the magnetic field, resulting in a well-developed magnetic tail behind the planet. However, as the planet rotates, the magnetosphere configuration changes from pole-on with a cylindrically shaped magnetotail plasma sheet to a more normal planar plasma sheet. Because of this unique geometry and the timing of the flyby, the spacecraft did not cross the plasma sheet. The outbound magnetopause was located at a distance of about 72.3 R_N ; multiple bow shock crossings were observed near 161 R_N .

The maximum plasma density observed within the magnetosphere was 1.4 cm⁻³, the smallest observed by Voyager in any magnetosphere. The plasma has at least two components, one consisting of light ions (mass 1 to 5 amu) and one of heavy ions (mass 10 to 40 amu). Most of the plasma is concentrated in a plasma sheet near the planet. The most likely source for the light ions is Neptune's atmosphere; the heavy ions probably escape from Triton.

The trapped particle population includes atomic hydrogen, singly ionized molecular hydrogen, and helium, with relative abundances of 1300:1:0.1. Higher energy

(>150 keV) electrons and ions exhibit steep gradients just inside the 14.3- R_N orbit of Triton. This and other factors suggest that Triton plays a determining role in controlling the outer regions of the Neptune magnetosphere. Near closest approach, soft particle fluxes resembling those in Earth's auroral zone were observed. Significant fluxes of energetic (≥ 1 MeV) trapped electrons and protons were measured within the magnetosphere. Maximum intensities occur near an L -shell value of 7, decreasing inward as a result of particle absorption by satellites and ring particles. Several distinct particle absorption features are seen in the electron and proton fluxes measured by Voyager. 1989N1 is easily identified as one of the absorbers, but, because of the complexity of the magnetic field, further analysis will be needed before closer absorption features can be attributed to specific satellites or rings. Protons have lower fluxes than electrons throughout the magnetosphere.

Although radio bursts from Neptune were first noted about 8 days before closest approach, later identifications of such bursts were possible in data taken as early as 30 days before closest approach. These bursts of radio emission were strongly polarized and occurred in the frequency range 100 to 1300 kHz with an unchanging periodicity of 16.11 hours. These are interpreted as originating in the vicinity of the south magnetic pole and having the characteristics of an omnidirectional radio strobe.

A more continuous type of smooth emissions was detected in the frequency range 20 to 865 kHz. Although the basic periodicity of 16.11 hours also applies to these emissions, a phase shift of about 180° was noted as the spacecraft passed the planet. The polarization of these emissions was variable within any given epoch, but the pattern repeated each planetary rotation. Here the interpretation is one of a narrow rotating radio beam being swept periodically across the spacecraft detectors.

No evidence exists for Neptune electrostatic discharges of the kind seen by PRA at Saturn and Uranus. Many typical plasma waves were detected by PWS during the encounter. These included electron plasma oscillations in the solar wind upstream of the bow shock, electrostatic turbulence at the bow shock, and chorus, hiss, electron cyclotron waves, and upper hybrid resonance waves in the inner magnetosphere. Preliminary analysis shows no plasma wave signature of an interaction of Triton with the magnetosphere, but the flyby geometry was not ideal for such observations. There is also no indication of lightning-generated whistlers.

The future of Voyager 2. As detailed analysis

of the results from the Voyager 2 Neptune encounter progresses over the next few years, it is expected that our understanding of Neptune and its rings, satellites, and magnetosphere will continue to grow. In the meantime, the two Voyager spacecraft will continue to explore the charged particle and magnetic field environment beyond the planets, perhaps encountering the solar wind termination shock, where the solar wind slows abruptly from supersonic to subsonic, and the heliopause, the boundary between the subsonic solar plasma and the interstellar wind. If both spacecraft continue to operate as well in the future as they have in the past, they should have sufficient electrical power and attitude control fuel to continue transmitting data until at least 2015. By that time Voyager 1 will be 129 astronomical units (AU) and Voyager 2 will be 107 AU from the sun, and both may be in the interstellar medium.

REFERENCES AND NOTES

1. For a discussion of the spacecraft, mission design criteria, trajectory selection, and the scientific investigations, see *Space Sci. Rev.* **21**, 75–376 (1977). A description of the design of the Voyager spacecraft is given in R. F. Draper, W. I. Purdy, G. Cunningham, paper 75-1155 presented at the American Institute of Aeronautics and Astronautics–American Geophysical Union Conference on the Exploration of the Outer Planets, St. Louis, 17 to 19 September 1975.
2. Voyager 1 Jupiter results are outlined in: *Science* **204**, 945–1008 (1979); *Nature* **280**, 725–806 (1979); *Geophys. Res. Lett.* **7**, 1–68 (1980). Voyager 2 Jupiter results are outlined in *Science* **206**, 925–996 (1979). Combined Voyager Jupiter results are contained in *J. Geophys. Res.* **85**, 8123–8841 (1981).
3. Voyager 1 Saturn results are outlined in: *Science* **212**, 159–243 (1981); *Nature* **292**, 675–755 (1981). Voyager 2 Saturn results are outlined in *Science* **215**, 499–594 (1982). Combined Voyager Saturn results are contained in *J. Geophys. Res.* **88**, 8625–9018 (1983). See also two special issues of *Icarus* [**53**, 163–387 (1983); **54**, 159–360 (1983)]; T. Gehrels and M. S. Matthews, Eds., *Saturn* (Univ. of Arizona Press, Tucson, 1984); R. Greenberg and A. Brahic, Eds., *Planetary Rings* (Univ. of Arizona Press, Tucson, 1984).
4. Voyager 2 Uranus results are outlined in *Science* **233**, 39–109 (1986); *J. Geophys. Res.* **92**, 14, 873–15,375 (1987). See also J. T. Bergstrahl and E. D. Miner, Eds., *Uranus* (Univ. of Arizona Press, Tucson, in press).
5. H. B. Hammel *et al.*, *Science* **245**, 1367 (1989).
6. H. J. Reitsemma *et al.*, *ibid.* **215**, 289 (1982); C. E. Couvaut *et al.*, *Icarus* **67**, 126 (1986); W. B. Hubbard *et al.*, *Nature* **319**, 636 (1986); P. D. Nicholson *et al.*, in preparation.
7. J. B. Pollack *et al.*, *Icarus* **37**, 587 (1979); P. Farinella *et al.*, *ibid.* **44**, 810 (1980); W. B. McKinnon, *Nature* **311**, 355 (1984); P. Goldreich *et al.*, *Science* **245**, 500 (1989); W. B. McKinnon and A. C. Leith, *Icarus*, in press.
8. We wish to pay special tribute to the members of the Voyager project team, without whom the data reported in these papers could not have been collected. The Voyager program is one of the programs of the Solar System Exploration Division of NASA's Office of Space Science and Applications. The Voyager project is managed by the Jet Propulsion Laboratory of the California Institute of Technology under contract with NASA.

27 October 1989; accepted 15 November 1989